

μm - and nm-Sized Catalytic Structures in Heat Sources for Thermoelectric Generators

L. I. Anatyshchuk^{1,*}, V. Ya. Mykhailovsky^{1,†}, L. T. Strutynska¹, M. V. Maksymuk¹,
V. V. Antoniuk¹, U. Burkhardt², W. Carrillo-Cabrera², and Yu. Grin^{2,*}

¹*Institute of Thermoelectricity, 58029 Chernivtsi, Ukraine*

²*Max-Planck-Institut für Chemische Physik fester Stoffe, 01187 Dresden, Germany*

Micro- and nano-structural organization and its influence on the efficiency of catalysts used in the heat sources for permeable thermoelectric generators were investigated. Two types of catalyst were studied—elemental platinum on aluminum oxide granulate Pt/Al₂O₃ and mixed transition-metal catalyst on fibrous silicon dioxide Co–Cr–Pd–Sr/SiO₂. The distribution of active components in catalytic structures which contribute to the maximum combustion completeness of organic fuel in heat sources was investigated. Practically full conversion of hydrocarbons was achieved already with 1 mass.% of platinum in the Pt/Al₂O₃ catalyst with sub- μm - and nm-sized particles placed at the input of the gas-air mixture into the channel of the permeable thermoelement. The propane-butane conversion rate of 97% for the catalyst Co–Cr–Pd/SiO₂ with was further enhanced by addition of 0.5 mass.% of Sr. The catalytic centers are formed by CoCr₂O₄ nanocrystals (10 to 40 nm in size) with Pd promotor in form of single crystals on the fibrous SiO₂ matrix.

Keywords: Catalysts, Combustion of Organic Fuel, Thermoelectric Generator, Heat Source.

1. INTRODUCTION

Combustion of liquid and/or gaseous fuels on solid catalysts is one of the most promising ways of obtaining heat to be used in thermoelectric generators. It allows significant elimination of heat losses with products of reaction, on the one hand, and formation of hazardous substances like CO, NO_x and fine-dispersed carbon, resulting from incomplete fuel combustion, on the other hand.¹ Noble metals Pt, Pd, Ir, Rh and multi-component oxides of transition metals Co, Cr, Fe, Ni, Cu with the general composition Me(I)Me₂(II)O₄ and the spinel-type crystal structure are studied and employed as active components of the catalysts for the complete combustion of both liquid and gas hydrocarbonic fuels.²

Two types of catalytic structures are predominantly used in heat sources of thermoelectric generators: (i) solid or granulated structures where the catalytically active component is deposited on the porous carriers (alumina, aluminosilicates); (ii) fibrous structures where

active components based on either noble metals or oxides of variable valency metals are deposited onto siliceous fiber. Of special interest for use in thermogenerators are permeable thermoelements with internal catalytic heat sources.³ Such thermoelements have pores or channels where the catalyst is located. Provided gas fuel in channels or pores is combusted such catalysts become embedded heat sources.

The catalytic heat sources properties for such kind of thermoelements are generally regulated by the concentration, nature and structure of the catalytically active material, as well as the geometry of channels where the catalyst is planted. Therefore, the enhancement of the catalyst efficiency and, hence, that of the catalytic heat source, it is of great practical importance. This justifies also the research on the spatial organization of the really working catalysts and on the effect of their nature and distribution of active components in them on the efficiency.⁴

The objective of the present paper is to study the micro- and nano-structural organization as well as distribution of catalytically active components in two catalyst types—elemental platinum on aluminum oxide granulate Pt/Al₂O₃

*Authors to whom correspondence should be addressed.

†Dr. Mykhailovsky passed away.

and mixed transition-metal catalyst on fibrous silicon dioxide Co–Cr–Pd–Sr/SiO₂—which are implemented to ensure maximum combustion rate of the gaseous hydrocarbon fuel in catalytic heat sources for permeable thermoelectric generators.

2. EXPERIMENTAL DETAILS

2.1. Materials

All reagents employed for preparation of catalysts were of analytical grade of purity and were used without additional treatments.

2.2. Preparation

The granulated catalyst was prepared by the impregnation of the alumina granulate (Al₂O₃) with the solution of H₂PtCl₆ with appropriate concentration.³ To control the impregnation depth of platinum, granulate was pre-treated with a vapor of organic solvent acetone (30 min). After impregnation, the granulate material was calcined in air at 550 °C for 2.5–3 hours.

The fibrous catalyst was prepared by the impregnation of the siliceous fiber (SiO₂) with the solutions of nitrate salts (Co(NO₃)₃ × 6H₂O, Cr(NO₃)₃ × 9H₂O) with appropriate concentration.³ To generate a catalyst promotor, the solution of PdCl₂ of the suitable concentration was added to the impregnating mixture of transition metals nitrates. Strontium stabilizer was added in form of Sr(NO₃)₂ × 4H₂O. After impregnation, the fibrous material was calcined in air at 550 °C for 1 hour.

2.3. Characterization

Phase identification was realized by powder X-ray diffraction experiments (Huber image plate Guinier camera G670) employing CuK α 1 radiation, $\lambda = 1.540562 \text{ \AA}$. Profile analysis and lattice parameters refinement were made with the program package WinCSD.⁵

The microstructure of the catalysts was investigated with the scanning electron microscope Philips XL30 using secondary and back-secondary techniques. The chemical composition was determined at different points on the surface of the powdered samples by energy-dispersive X-ray spectroscopy (EDXS) with an Si(Li) detector attached to the scanning electron microscope. For the quantification, the scattered electrons procedure was employed.

The local structure of the catalysts was characterized by transmission electron microscopy experiments. The electron microscope FEI Tecnai 10 used in this study was operated at 100 kV.

2.4. Modelling

Computer simulation of the temperature distribution within the permeable thermoelectric module was performed using the finite elements technique implemented into the COMSOL Multiphysics software.⁶

3. RESULTS AND DISCUSSION

Optimal use of a catalyst depends on the proper choice of the temperature window and spatial conditions for the combustion process. Therefore temperature distribution in the channel and in thermoelectric material within a permeable thermoelectric module was first modeled for three thermoelements configurations (Fig. 1):

—thin layer of the catalyst (200 μm) is deposited onto the walls of cylindrical channels in the legs of a thermoelectric element;

—channels of a thermoelement are filled with the porous catalyst (particle size 200–250 μm) with regular active component distribution along the volume of the channel;

—active catalytic element is placed at the input of the gas-air mixture into the channel which is filled with porous carrier (Al₂O₃).

It is assumed in calculations that the active component concentration is equal for all three variants. The completeness of gas combustion is also considered to be the same which is controlled by the speed of gas/air flow through the channel. The thermal conductivity of the thermoelectric material is assumed to be within the range of 0.012–0.016 W cm⁻¹ K⁻¹. Elemental Pt and Pd are used as models for the catalytically active phase.

The maximum temperature difference between the cold and hot sides of the leg is obtained if the catalyst is placed in the input part of the channel (gas flow direction is marked with arrow, Fig. 1(a)), while the regular distribution of the catalyst in the channel volume is less effective (Fig. 1(b)). The catalyst deposition onto the inner walls of the cylindrical channels is the least efficient (Fig. 1(c)). The modelling yields the temperature window for the catalytic combustion between 500 and 600 °C.

The catalysts with the regular distribution of the active centers on surface and/or in volume of the carrier matrix may be prepared on base of the porous granulated Al₂O₃ or the fibrous silica. Such structures enable catalytic heat generation in the external diffusion regime on the surface-distributed active centers, and/or in the intrinsic diffusion

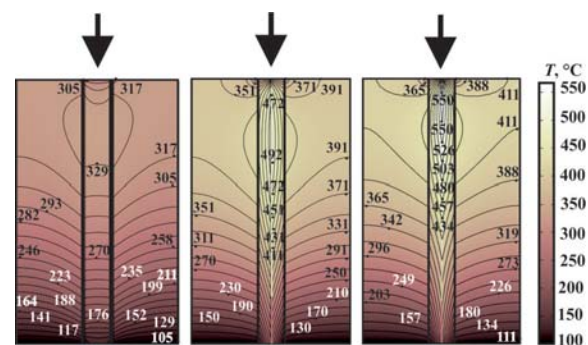


Figure 1. Temperature distribution (in °C) in a cylindrical leg of the permeable thermoelectric element: height of leg is 20 mm; diameter of channel is 2 mm; diameter of leg is 12 mm.

regime in case of the volume distribution. The maintaining of the spatial distribution of the catalytically active centers is the way for optimization of the fuel combustion rate and increasing the efficiency of heat sources for permeable thermoelectric generators.

An important property of Al_2O_3 -based carriers for the catalysts obtained with the impregnation technique is the number of hydroxyl groups adsorbed on the active surfaces of the carrier.^{7,8} The thermal pre-treatment of the Al_2O_3 -based carrier allows to control this number and — thus — has a significant effect on the catalyst efficiency during the reaction of gas fuel catalytic oxidation. The temperature range of 300–400 °C was found to be the optimal regime to provide the necessary number of adsorbed hydroxyl groups on the carrier surface. A further increase in the carrier heating temperature causes the decrease in fuel combustion completeness due to the significant decrease in active acid centers concentration with increasing calcination temperature.⁹

Volume distribution of the active component in the porous Al_2O_3 based carrier can be further controlled by the time of pre-treatment of the carrier with the vapor of organic solvents.² Depending on the pre-treatment, different types of active component distribution can be targeted. The uniform active component distribution in the porous carrier volume provides for the maximum degree of gas conversion in the internal diffusion regime with low flow rate of the combustible mixture, where the hydrocarbons concentration is high enough. The surface distribution ensures the maximum degree of hydrocarbons conversion in the external diffusion regime when the flow rate of combustible mixture is very high. The essential mechanism of the influence of the evaporating solvent is its competitive adsorption on the carrier surface² resulting in the considerable increase of the active component transport (H_2PtCl_6 or PdCl_2 for this case) to the volume of the porous carrier.¹⁰ For the catalysts investigated in this study, the organic solvent pre-treatment was maintained with the aim of work with the high flow rate of the combustion mixture.

The X-ray powder diffraction pattern of the $\text{Pt}/\text{Al}_2\text{O}_3$ catalyst obtained in this study (Fig. 2) shows only reflections of the $\gamma\text{-Al}_2\text{O}_3$ carrier and elemental platinum. Obviously, platinum hydrochloric acid decomposes during the calcination stage of the catalyst manufacturing and yields the element. The refined lattice parameter of platinum in the catalyst $a = 3.937(8)$ Å is close to the literature values.¹¹ The large half-widths of the diffraction peaks suggest very small size of the diffraction domains of the order of 10 nm. This is confirmed by the investigation of the microstructure. The catalyst spatial structure is presented in Figure 3 (scanning electron microscope in back-scatter mode). Small Pt particles with the size 0.1–1.5 μm are uniformly distributed in the $\gamma\text{-Al}_2\text{O}_3$ matrix. Taking into account the X-ray diffraction data, these particles are

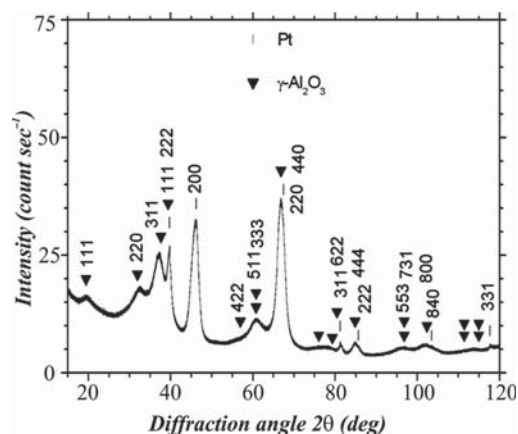


Figure 2. Powder X-ray diffraction pattern of the $\text{Pt}/\text{Al}_2\text{O}_3$ catalyst ($\text{CuK}\alpha 1$ radiation, $\lambda = 1.540562$ Å). Reflections of $\gamma\text{-Al}_2\text{O}_3$ and elemental platinum are indexed (ICSD data base, nos. 76153 for Pt and 66550 for $\gamma\text{-alumina}$ ¹¹).

composed from the smaller nm-sized diffraction domains. The $\gamma\text{-Al}_2\text{O}_3$ matrix has a loose organization and consists of particles of size up to 10 μm .

The efficiency of Pt catalysts with the volume distribution of active phase and the spatial organization described above was studied in the deep oxidation reaction of the propane-butane mixture (with the ratio of 4:1) in the catalytic heat source for thermogenerator with the power between 10 and 100 W. The combustion products analysis (the completeness of fuel combustion) was performed by gas chromatography. The maximum combustion temperature and hydrocarbons conversion rate were chosen as efficiency criteria (Fig. 4). The maximum oxidation temperature was within the range of 470–510 °C, whereas conversion approached 100%. The optimal platinum concentration was found in the range of 0.5–1.5% of the carrier mass.

X-ray powder diffraction pattern of the $\text{Co-Cr-Pd}/\text{SiO}_2$ catalyst with the composition of Co–Cr (29 mass%) and

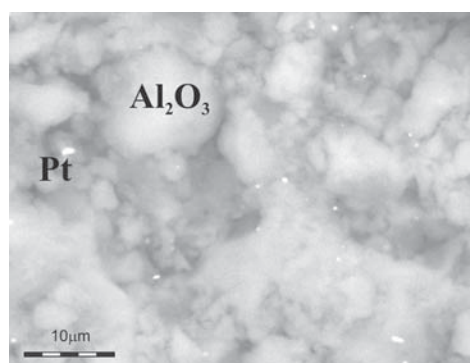


Figure 3. Spatial organization of the $\text{Pt}/\gamma\text{-Al}_2\text{O}_3$ catalyst (back-scatter SEM image). The sub-micrometer- and nm-sized particles of elemental platinum (white spots) are uniformly distributed in the $\gamma\text{-Al}_2\text{O}_3$ matrix.

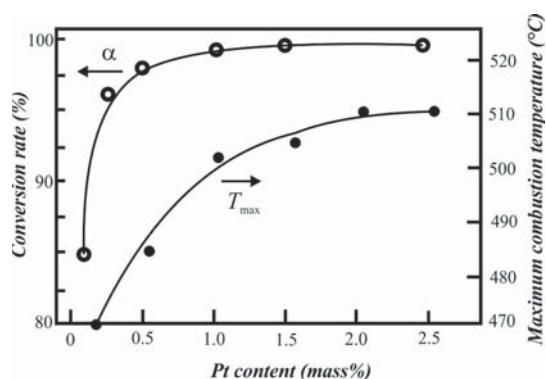


Figure 4. Hydrocarbons conversion rate (α) and maximum combustion temperature (T_{\max}) versus the Pt content in the Pt/Al₂O₃ catalyst.

Pd (0.2 mass%) — prepared as described in Experimental details — shows the presence of a crystalline phase CoCr₂O₄ with the spinel-type of crystal structure (Fig. 5). Decomposition of the initial nitrates of cobalt and chromium results in the formation of corresponding oxides that react to the triple spinel phase during the calcination.¹² Due to the initially small palladium concentration the reflections of elemental palladium or palladium oxide(s) in the powder X-ray diffraction patterns were not observed. The refined lattice parameter of the CoCr₂O₄ spinel phase is $a = 8.346(3)$ Å, being close to the literature data.¹¹ Analysis of the available reflections applying the Scherrer equation reveals diffraction domains of the size of order 20 nm.

Transmission electron microscope study revealed indeed the presence of CoCr₂O₄ nanocrystals (10 to 40 nm in size) being agglomerated around large particles of amorphous SiO₂ (Figs. 6(a, b)). These nanocrystals serve obviously as the diffraction domains (cf. above). The lattice parameter $a = 8.3$ Å obtained from the electron diffraction (Fig. 6(c)) is in agreement with the data on the X-ray powder diffraction data. The condensed nanocrystals are agglomerated on

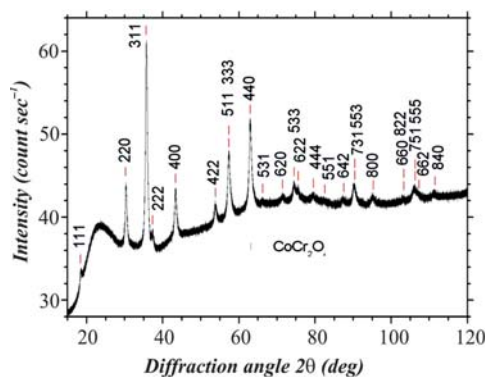


Figure 5. Powder X-ray diffraction pattern of the Co-Cr-Pd/SiO₂ catalyst (CuK α 1 radiation, $\lambda = 1.540562$ Å). Reflections of CoCr₂O₄ phase with the spinel-type crystal structure are indexed (ICSD no. 61612¹¹).

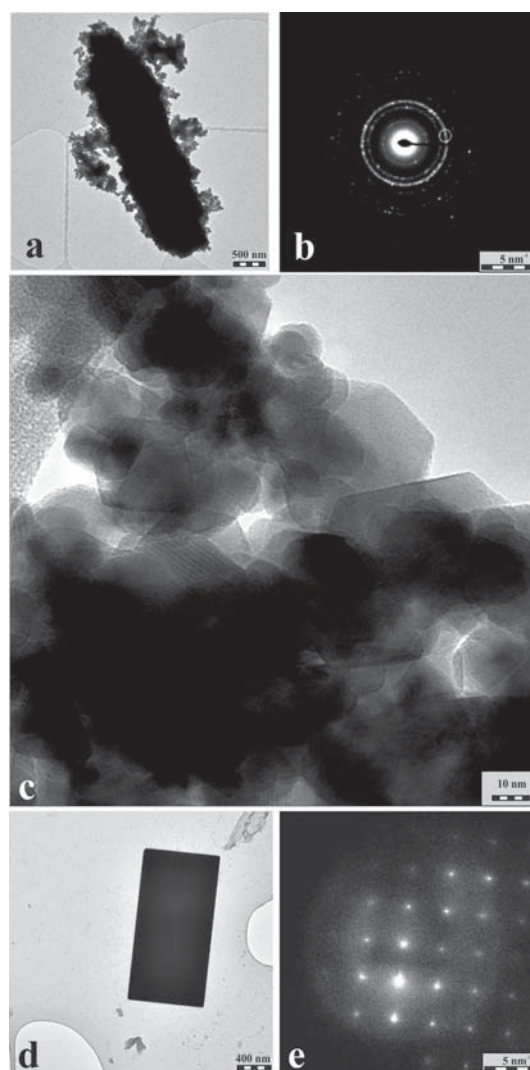


Figure 6. Transmission electron microscopy images of the Co-Cr-Pd/SiO₂ catalyst: (a) amorphous SiO₂ particle with agglomerated CoCr₂O₄ nanocrystals; (b) electron diffraction pattern of the CoCr₂O₄ nanocrystals; (c) general view of the catalyst nanocrystals; (d) micro-crystal of Pd; (e) electron diffraction pattern along [001] direction of the Pd micro-crystal in (d) with the characteristic interplanar distance of $d_{110} = 2.78$ Å (corresponding spot observed due to dynamical multi-beam effects).

the surface of large SiO₂ particles (Fig. 6(d)). Palladium promotor was found in the form of individual micro- and nano-crystals situated between CoCr₂O₄ nanocrystals (Figs. 6(e, f)).

Taken into account the results obtained on the catalytically active phases and their organization in the Co-Cr-Pd/SiO₂ catalyst, a series of catalysts with fibrous structure was developed on the base of cobalt and chromium oxides with palladium. To stabilize the active phase of the catalyst, Sr additives were used. They hamper the cobalt-chromium spinel decomposition into Co and Cr oxides.

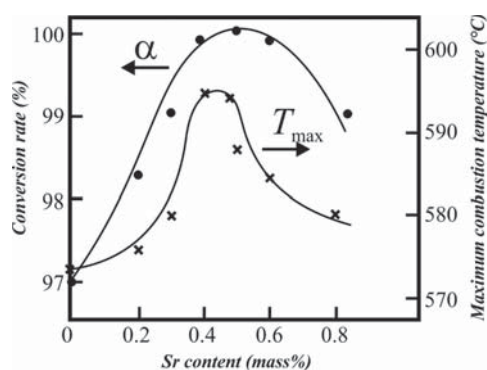


Figure 7. Propane-butane conversion rate (α) and the maximum combustion temperature (T_{\max}) versus Sr content (x) in the catalyst Co–Cr(29.0)–Pd(0.2)–Sr(x)/SiO₂.

As a result the catalyst deactivation is reduced resulting in the prolonged operation of a heat source.

The Co–Cr–Pd–Sr/SiO₂ catalysts were studied in the heat source with gas flow of 0.12 g/h·cm³. The maximum combustion temperature and the hydrocarbons conversion rate were chosen as the efficiency criteria (Fig. 7). Already the strontium-less catalyst with 29 mass.% of chromium and 0.2 mass.% of palladium allows to achieve the combustion rate of 97 %. The Sr concentrations up to 1 mass.% were studied for their influence of the catalytic efficiency. At strontium content of 0.4–0.6 mass. %, the maximal process temperature (close to 600 °C) and the rate of the gas fuel oxidation near 100% were obtained. Such spinel phase CoCr₂O₄ based catalyst remains stable after 8000 hours of the continuous heat source operation being the main factor of the stability of the power production in the permeable thermoelectric generator.

4. CONCLUSIONS

For the developed permeable thermoelements, the maximum temperature difference between the hot and the cold sides during gas combustion in a thermoelement with the internal catalytic heat source was obtained by surface distribution of the catalytically active component. It was placed at the input point of the gas-air mixture into the channel of a permeable thermoelement.

The study of catalysts on granulated Al₂O₃ carrier showed that platinum is uniformly distributed in the carrier

matrix and is there in the elemental state. This is a result of thermal decomposition of the initial platinum compounds with a subsequent reaction of platinum oxide with hydrogen. Platinum agglomerates have sub- μm size and contains diffraction domains with the size of order of 10 nm. With such organization of catalyst, the practically full combustion was achieved with 0.5–1.5 mass.% of platinum.

X-ray powder diffraction study showed that the Co–Cr–Pd/SiO₂ catalyst (silica fiber), obtained by the impregnation method, contains mainly the nano-crystalline (particle size 10–40 nm) spinel phase CoCr₂O₄ distributed on the amorphous SiO₂. The palladium promotor is found in the form of individual sub- μm single crystals situated close to CoCr₂O₄ nanocrystals. Already without any additives, such catalyst (29 mass.% of Cr and 0.2 mass.% of Pd) yields 97 % of combustion for the propane-butane fuel mixture. Further Sr addition results in the practically full combustion.

Acknowledgments: The authors are indebted to Dr. A. Levin for valuable technical assistance by performing the X-ray powder diffraction experiments.

References and Notes

1. V. Ya. Mykhailovsky, *Proc. Nat. Acad. Sci. Ukraine. Energetics* 4, 111 (2002).
2. T. G. Alkhazov and L. Ya. Margolis, *Deep Catalytic Oxidation of Organic Substances*, Chemistry, Moscow (1985).
3. V. Ya. Mykhailovsky, *Organic Fueled Thermoelectric Generators*, Habilitation Thesis, Chernivtsi (2007).
4. M. D. Argyle and C. H. Bartholomew, *Catalysts* 5, 145 (2015).
5. L. Akselrud and Yu. Grin, *J. Appl. Crystallogr.* 47, 803 (2014).
6. *Multiphysics Software Product Suite*, www.comsol.com.
7. A. W. Peters, *Patent EP 0354525 A1*, published 14.02. (1990).
8. G. V. Lisichkin, G. V. Kudriavtsev, A. A. Sedan, S. M. Staroverov, and A. Ya. Yuffa, *Modified Silica in Sorption, Catalysis and Chromatography*, Chemistry, Moscow (1986).
9. N. M. Popova, *Catalysts for the Automotive Exhaust Gases Purification*, Nauka, Alma Ata (1987).
10. Yu. V. Dubinin, N. A. Yazykov, A. D. Simonov, V. A. Yakovlev, A. A. Sarayev, V. V. Kaichev, O. A. Bulavchenko, A. V. Ischenko and V. V. Mokrinsky, *Kataliz v Promyshlennosti (Catalysis in Industry)* 4, 68 (2013), in Russian.
11. *Inorganic Crystal Structure Data Base*, version 3.3.0, FIZ Karlsruhe (2014).
12. N. V. Shishkina, A. A. Gavrilov, V. A. Ushakov, and Z. P. Ismagilov, *Chemical Engineering* 5, 31 (2013).

Received: 14 March 2016. Revised/Accepted: 5 May 2016.